

A Random-Feature Based Newton Method for Empirical Risk Minimization in Reproducing Kernel Hilbert Space

Ting-Jui Chang and Shahin Shahrampour

Texas A&M University

E-mail: tingjui.chang@tamu.edu, shahin@tamu.edu

Abstract

In supervised learning using kernel methods, we encounter a large-scale finite-sum minimization over a reproducing kernel Hilbert space (RKHS). Often times large-scale finite-sum problems can be solved using efficient variants of Newton's method where the Hessian is approximated via sub-samples. In RKHS, however, the dependence of the penalty function to kernel makes standard sub-sampling approaches inapplicable, since the gram matrix is not readily available in a low-rank form. In this paper, we observe that for this class of problems, one can naturally use kernel approximation to speed up the Newton's method. Focusing on randomized features for kernel approximation, we provide a novel second-order algorithm that enjoys local superlinear convergence and global convergence in the high probability sense. The key to our analysis is showing that the approximated Hessian via random features preserves the spectrum of the original Hessian. We provide numerical experiments verifying the efficiency of our approach, compared to variants of sub-sampling methods.

1 Introduction

At the heart of many (supervised) machine learning problems, a learner must solve the following risk minimization

$$\min_{\mathbf{w} \in \mathbb{R}^d} \left\{ F(\mathbf{w}) \triangleq \sum_{i=1}^n \ell(y_i, f(\mathbf{x}_i; \mathbf{w})) + \lambda R(\mathbf{w}) \right\}, \quad (1)$$

where $\{(\mathbf{x}_i, y_i)\}_{i=1}^n$ are input-output data samples generated independently from an unknown distribution, ℓ is a task-dependent loss function, and R is a regularizer. Furthermore, f is a certain function class, parameterized by \mathbf{w} , on which the learner wants to minimize the risk. As an example, for linear models we simply have $f(\mathbf{x}; \mathbf{w}) = \mathbf{x}^T \mathbf{w}$.

First-order optimization algorithms have been widely used to solve large-scale optimization problems of form (1) (e.g., see (1) for a recent review). Relying solely on the gradient information, these methods

converge to (local) optima. However, second-order algorithms employ the curvature information to properly re-scale the gradient, resulting in more appropriate directions and much faster convergence rates. As an example, in the unconstrained optimization, Newton’s method pre-multiplies the gradient by Hessian inverse at each iteration. It is quite well-known that under some technical assumptions, Newton’s method can achieve a locally super-linear convergence rate (see e.g., Theorem 1.2.5 in (2)). However, the cost of Hessian inversion is the major drawback of Newton’s method in practice.

To improve the (per iteration) time complexity, various approaches have been explored in the literature for approximately capturing the Hessian information. Popular methods in this direction include sub-sampling the Hessian matrix (3–5), sketching techniques (6), as well as quasi-Newton methods (7–10) and its stochastic variants (11–13).

Nevertheless, when the function class of f in (1) is a reproducing kernel Hilbert space (RKHS), due to the special structure of the problem, some of the aforementioned methods are not directly applicable and need some adjustments.

1.1 Risk Minimization in RKHS

In this paper, we restrict our attention to risk minimization in the case that the function f in (1) belongs to RKHS. In particular, consider a symmetric positive-definite function $k(\cdot, \cdot)$ such that $\sum_{i,j=1}^n \alpha_i \alpha_j k(\mathbf{x}_i, \mathbf{x}_j) \geq 0$ for $\boldsymbol{\alpha} = [\alpha_1, \dots, \alpha_n]^T \in \mathbb{R}^n$. Then, $k(\cdot, \cdot)$ is called a positive (semi-)definite kernel and can define a Hilbert space \mathcal{H} where $f(\mathbf{x}; \mathbf{w}) = \sum_{i=1}^n w_i k(\mathbf{x}, \mathbf{x}_i)$. This class of functions forms the basis of kernel methods that are powerful tools for data representation and are commonly used in machine learning (14). In this scenario, the objective function takes the following form

$$F(\mathbf{w}) = \sum_{i=1}^n \ell\left(y_i, \sum_{j=1}^n w_j k(\mathbf{x}_i, \mathbf{x}_j)\right) + \frac{\lambda}{2} \|f\|_{\mathcal{H}}^2, \quad (2)$$

where the regularizer in (1) is the RKHS norm. Let us denote the kernel (gram) matrix as $[\mathbf{K}]_{ij} = k(\mathbf{x}_i, \mathbf{x}_j)$. The definition of inner product in RKHS immediately implies that $\|f\|_{\mathcal{H}}^2 = \mathbf{w}^T \mathbf{K} \mathbf{w}$ (see e.g., page 62 of (14)). Then, assuming that ℓ is twice-differentiable, the Hessian of the objective function in

(2) can be calculated as follows

$$\mathbf{H}(\mathbf{w}) \triangleq \nabla^2 F(\mathbf{w}) = \mathbf{K}\mathbf{D}(\mathbf{w})\mathbf{K} + \lambda\mathbf{K}, \quad (3)$$

where $\mathbf{D}(\mathbf{w}) \in \mathbb{R}^{n \times n}$ is a diagonal matrix defined as

$$[\mathbf{D}(\mathbf{w})]_{ii} = \ell''\left(y_i, \sum_{j=1}^n w_j k(\mathbf{x}_i, \mathbf{x}_j)\right). \quad (4)$$

Observe that in (3), the diagonal structure of $\mathbf{D}(\mathbf{w})$ and symmetry of \mathbf{K} entails that $\mathbf{K}\mathbf{D}(\mathbf{w})\mathbf{K}$ can be trivially represented as a sum of rank-one matrices. However, \mathbf{K} , which appears as a result of the regularization term, may be dense and not readily available in a low-rank form. In other words, decomposing \mathbf{K} to a low-rank matrix also requires effort, so we cannot directly apply sub-sampling Newton techniques, such as those in (3–5) to optimize the objective function (2). This naturally raises the following question, which we pursue in this paper:

Problem 1 *Given the explicit connection of the Hessian (3) to the gram matrix \mathbf{K} , can we use kernel approximation techniques to speed up the Newton method?*

1.2 Our Contributions

In this paper, we answer to Problem 1 in the affirmative by providing the following contributions:

- We apply the idea of randomized features for kernel approximation (15) to approximate the Hessian (3). Our algorithm is thus dubbed Random-Feature based Newton (RFN).
- The key to our technical analysis is Lemma 2, which shows that when enough random features are sampled, the approximate Hessian is close to $\mathbf{H}(\mathbf{w})$ in the spectral norm sense. Our analysis relies on matrix concentration inequalities rather than refining standard guarantees in the kernel approximation literature.
- We prove that RFN enjoys local superlinear convergence and global convergence in the high probability sense.

- Our numerical experiments on benchmark datasets provide a performance comparison among RFN, classical Newton, L-BFGS, and a variation of sub-sampled Newton methods (as they are not directly applicable to (2)). We illustrate that RFN achieves a superior loss vs. run-time rate against its competitors. We also investigate the sensitivity of RFN with respect to a number of hyper-parameters.

1.3 Related Literature

Inspired by the success of stochastic first-order algorithms for large-scale machine learning, the stochastic forms of second-order optimization have received more attention in the recent literature. In this section, we will discuss several stochastic second-order methods and we split them into two categories: quasi-Newton methods and second-order Hessian-based methods.

Quasi-Newton Methods: Instead of doing the expensive computation of the Newton step, quasi-Newton methods approximate the Hessian by using the information obtained from gradient evaluations. BFGS algorithm (7–10) is a seminal work of this type. Recent works (11–13) in this area has focused on stochastic quasi-Newton methods to obtain curvature information in a computationally inexpensive manner. An interesting advancement in this line of work was provided by (16) who proposed an algorithm based on L-BFGS by incorporating ideas from variance reduction to achieve linear convergence to the optimum.

Second-Order Hessian based Methods: One of the appealing features of Newton’s method is its linear-quadratic convergence rate. However, there are two main issues for the implementation of the classical Newton method: the cost of Hessian construction, and the cost of Hessian inversion. For instance, in application to the family of generalized linear models (GLMs) involving an $n \times d$ data matrix, the computation of the full Hessian costs $O(nd^2)$ and the matrix inversion takes $O(d^3)$ time. This high cost for modern machine learning applications motivates researchers to apply randomization techniques, and thus sub-sampled Newton methods have gained a lot of attention recently.

The pioneering work in (17, 18) establishes the convergence of the modified Newton’s method with sub-sampled Hessian. Under a similar setting to (17, 18), the work of (19) provides modifications in order to get better estimated Hessian and time cost performance. Within the context of deep neural networks, (20) proposes a sub-sampled Gauss-Newton method for the training and studies the choice of the regularization parameter.

(21) proposes a Newton-like method, where the Hessian is approximated first by sub-sampling the true Hessian and then computing its truncated eigenvalue decomposition. Their work establishes non-asymptotic local convergence rates for the uniform sub-sampling of the Hessian. (6) proposes another Hessian approximation method, called Newton sketching, which approximates the true Hessian through random projection matrices. This method is applicable for the case where the square root of the full Hessian is available and the best complexity results are achieved when the randomized Hadamard transform is used.

(3, 4) analyze the global and local convergence rates for sub-sampled Newton methods with different sampling rates for gradient and Hessian approximations. (3) shows their convergence results in expectation whereas (4) provides high probability guarantees by applying matrix concentration inequalities (22, 23). The work of (4) further relaxes a common assumption in the literature: though the objective function is assumed to be strongly convex, the individual functions are only weakly convex. Along this line of works, (5) builds the approximated Hessian by applying non-uniform sampling based on the data matrix to get better dependence on problem specific quantities.

(24) proposes a method to compute an unbiased estimator of the inverse Hessian based on the power expansion of the Hessian inverse. The method achieves a time complexity scaling linearly with the size of variables. This is followed by an improved and simplified convergence analysis in (25).

The main distinction of our work with prior art is that we consider minimization in RKHS, where there are explicit connections between the Hessian and the gram matrix. We leverage this fact to approximate the Hessian, and we provide theoretical guarantees for our method.

2 Random-Feature Based Newton Method

2.1 Background on Random Features for Kernel Approximation

As discussed in the Introduction, the Hessian of the objective function in (2) can be written as $\mathbf{H}(\mathbf{w}) = \mathbf{K}\mathbf{D}(\mathbf{w})\mathbf{K} + \lambda\mathbf{K}$, where $[\mathbf{K}]_{ij} = k(\mathbf{x}_i, \mathbf{x}_j)$ is the gram matrix. The Hessian is a square matrix of size n and a plain inversion of that in Newton's method introduces a prohibitive cost of $O(n^3)$. To find a low-rank representation of Hessian, the key is to approximate the gram matrix $\mathbf{K} \in \mathbb{R}^{n \times n}$, which in general is dense. An elegant method for kernel approximation, called random Fourier features, was introduced in (15). Let $\tau(\boldsymbol{\omega})$ be a probability density with support $\Omega \subseteq \mathbb{R}^d$. Consider any kernel function with the following integral form

$$k(\mathbf{x}, \mathbf{x}') = \int_{\Omega} \phi(\mathbf{x}, \boldsymbol{\omega})\phi(\mathbf{x}', \boldsymbol{\omega})\tau(\boldsymbol{\omega})d\boldsymbol{\omega}, \quad (5)$$

where $\phi(\mathbf{x}, \boldsymbol{\omega}) : \mathbb{R}^d \rightarrow \mathbb{R}$ is a feature map. We can immediately see from (5) that the kernel function can be approximated via Monte-Carlo sampling as

$$k(\mathbf{x}, \mathbf{x}') \approx \frac{1}{m} \sum_{s=1}^m \phi(\mathbf{x}, \boldsymbol{\omega}_s)\phi(\mathbf{x}', \boldsymbol{\omega}_s), \quad (6)$$

where $\{\boldsymbol{\omega}_s\}_{s=1}^m$ are independent samples from the density $\tau(\boldsymbol{\omega})$ and are called *random features*. There exist many kernels taking the form (5), including shift-invariant kernels (15) and dot product (e.g., polynomial) kernels (26) (see Table 1 in (27) for an exhaustive list). Gaussian kernel, for example, can be approximated using $\phi(\mathbf{x}, \boldsymbol{\omega}) = \sqrt{2} \cos(\boldsymbol{\omega}^T \mathbf{x} + b)$ where $\boldsymbol{\omega}$ follows a Gaussian distribution and b has a uniform distribution on $[0, 2\pi]$.

We now define

$$\mathbf{z}(\boldsymbol{\omega}) \triangleq [\phi(\mathbf{x}_1, \boldsymbol{\omega}), \dots, \phi(\mathbf{x}_n, \boldsymbol{\omega})]^T. \quad (7)$$

Then, the gram matrix \mathbf{K} can be approximated with $\mathbf{Z}\mathbf{Z}^T$ where $\mathbf{Z} \in \mathbb{R}^{n \times m}$ is the following matrix

$$\mathbf{Z} \triangleq \frac{1}{\sqrt{m}} [\mathbf{z}(\boldsymbol{\omega}_1), \dots, \mathbf{z}(\boldsymbol{\omega}_m)]. \quad (8)$$

When $m < n$ in above, the approximation of \mathbf{K} is low-rank, saving computational cost when used to find the Newton direction. (28) prove the following ϵ -spectral approximation guarantee for $\mathbf{K} \approx \mathbf{Z}\mathbf{Z}^T$:

Theorem 1 (28) *Let $\epsilon \in (0, 1/2]$ and $\delta \in (0, 1)$ be fixed constants. Assume that $\|\mathbf{K}\|_2 \geq \gamma$. If we use $m \geq \frac{8}{3}\epsilon^{-2}\frac{n}{\gamma} \ln(16S_\gamma(\mathbf{K})/\delta)$ random Fourier features (sampled from $\tau(\boldsymbol{\omega})$), the following identity holds*

$$(1 - \epsilon)(\mathbf{K} + \gamma\mathbf{I}) \preceq \mathbf{Z}\mathbf{Z}^T + \gamma\mathbf{I} \preceq (1 + \epsilon)(\mathbf{K} + \gamma\mathbf{I}), \quad (9)$$

with probability at least $1 - \delta$, where $S_\gamma(\mathbf{K}) \triangleq \text{Tr}[\mathbf{K}(\mathbf{K} + \gamma\mathbf{I})^{-1}]$.

In view of (9), $\mathbf{Z}\mathbf{Z}^T + \gamma\mathbf{I}$ is dubbed an ϵ -spectral approximation of $\mathbf{K} + \gamma\mathbf{I}$. Theorem 1 characterizes the number of random features required to achieve a ϵ -spectral approximation of the kernel matrix given a specific γ . Nevertheless, if we apply this result to approximate the Hessian (3) in a plug-and-play fashion, the number of required features would be $m = \Omega(\epsilon^{-2})$. In Lemma 2, we establish a novel bound specifically for approximation of the Hessian $\mathbf{H}(\cdot)$, where the dependence has the potential to be improved to $m = \Omega(\epsilon^{-1})$.

2.2 Main Algorithm: Random-Featured Based Newton

We now leverage the random feature approximation, introduced in the previous section, for Hessian approximation. Following 3 and using the approximation $\mathbf{K} \approx \mathbf{Z}\mathbf{Z}^T$, where \mathbf{Z} is given in (8), we derive

$$\widehat{\mathbf{H}}(\mathbf{w}) = \mathbf{Z}\mathbf{Z}^T\mathbf{D}(\mathbf{w})\mathbf{Z}\mathbf{Z}^T + \lambda\mathbf{Z}\mathbf{Z}^T. \quad (10)$$

It is immediate that when $m < n$, the above approximated Hessian is singular, so in order to make $\widehat{\mathbf{H}}(\mathbf{w})$ invertible, a regularization term $\mu\mathbf{I}$ (for a some $\mu > 0$) is added to above, and the new approximate can be written as,

$$\widehat{\mathbf{H}}_\mu(\mathbf{w}) \triangleq \mathbf{Z}[\mathbf{Z}^T\mathbf{D}(\mathbf{w})\mathbf{Z} + \lambda\mathbf{I}]\mathbf{Z}^T + \mu\mathbf{I}. \quad (11)$$

Let $\mathbf{C}(\mathbf{w}) \triangleq \mathbf{Z}^T\mathbf{D}(\mathbf{w})\mathbf{Z} + \lambda\mathbf{I}$. By matrix inversion lemma, $\widehat{\mathbf{H}}_\mu^{-1}(\mathbf{w})$ can be written as

$$\widehat{\mathbf{H}}_\mu^{-1}(\mathbf{w}) = \frac{1}{\mu} \left[\mathbf{I} - \mathbf{Z} \left(\mu\mathbf{C}^{-1}(\mathbf{w}) + \mathbf{Z}^T\mathbf{Z} \right)^{-1} \mathbf{Z}^T \right], \quad (12)$$

which can reduce the time complexity of computing $\widehat{\mathbf{H}}_\mu^{-1}(\mathbf{w})\nabla F(\mathbf{w})$ from $O(n^3)$ to $O(m^2n)$.

Algorithm 1 Random-Feature Based Newton (RFN)

- 1: **Input:** Initial point \mathbf{w}_0 , # of iterations t_0 , # of random features m , distribution of random features $\tau(\omega)$, hyper-parameters for backtracking line search, regularization parameters $\lambda, \mu > 0$.
 - 2: **Output:** \mathbf{w}_{t_0}
 - 3: **for** $t = 0$ **to** $t_0 - 1$ **do**
 - 4: Sample m independent random features from τ and construct the feature matrix \mathbf{Z} as in (8).
 - 5: Compute $\mathbf{g}(\mathbf{w}_t) = \nabla F(\mathbf{w}_t)$, the gradient of the objective (2).
 - 6: Compute $\hat{\mathbf{H}}_\mu^{-1}(\mathbf{w}_t)$ as given in (12).
 - 7: Update $\mathbf{w}_{t+1} = \mathbf{w}_t - \alpha_t \hat{\mathbf{H}}_\mu^{-1}(\mathbf{w}_t) \mathbf{g}(\mathbf{w}_t)$, where α_t is selected via backtracking line search.
 - 8: **end for**
-

2.3 Adjustment of Sub-sampled Newton Methods

Sub-sampled Newton methods often end up working with Hessians of the form

$$\mathbf{H}(\mathbf{w}) = \frac{1}{n} \sum_{i=1}^n \mathbf{A}_i(\mathbf{w}) \mathbf{A}_i^T(\mathbf{w}) + \mathbf{Q}(\mathbf{w}),$$

where $\mathbf{A}_i(\mathbf{w})$ is a vector and $\mathbf{Q}(\mathbf{w})$ is a data-independent matrix (see e.g., (5)). Given this structure, if we randomly select a subset \mathcal{I} of data points, the Hessian can be approximated as

$$\hat{\mathbf{H}}(\mathbf{w}) = \frac{1}{|\mathcal{I}|} \sum_{i \in \mathcal{I}} \mathbf{A}_i(\mathbf{w}) \mathbf{A}_i^T(\mathbf{w}) + \mathbf{Q}(\mathbf{w}).$$

This would reduce the time cost of Hessian construction by a factor $|\mathcal{I}|/n$. Furthermore, since the approximated Hessian still consists of sum of rank-one matrices (in the data-related part), one can apply conjugate gradient (CG) method when computing the newton step to further speed up the process (3–5).

However, it turns out that the Hessian of the objective function 2, i.e., $\mathbf{K}\mathbf{D}(\mathbf{w})\mathbf{K} + \lambda\mathbf{K}$, cannot be directly handled by sub-sampling, since the regularizer in this case is indeed *data-dependent* and writing it as a sum of rank-one matrices requires a low-rank decomposition. In this case, sub-sampled Newton techniques can be adjusted using the Nyström method for column sampling (see e.g., (29) for a review on Nyström). Let $\mathcal{V} = \{1, \dots, n\}$ and \mathcal{I} denote a (random) subset of \mathcal{V} . Furthermore, denote by $\mathbf{K}(\mathcal{A}, \mathcal{B})$ the sub-matrix of \mathbf{K} with rows in $\mathcal{A} \subseteq \mathcal{V}$ and columns in $\mathcal{B} \subseteq \mathcal{V}$. Then, the gram matrix \mathbf{K} can be approximated as

$$\mathbf{K} \approx \mathbf{K}(\mathcal{V}, \mathcal{I}) \mathbf{K}(\mathcal{I}, \mathcal{I})^\dagger \mathbf{K}(\mathcal{I}, \mathcal{V}), \quad (13)$$

where \mathbf{M}^\dagger denotes the pseudo-inverse of \mathbf{M} . This decomposition introduces $O(n|\mathcal{I}|^2)$ time cost but circumvents the need for matrix inversion (by applying CG method). Notice that the first term of the Hessian can be trivially sub-sampled since

$$\mathbf{K}\mathbf{D}(\mathbf{w})\mathbf{K} = \sum_{i=1}^n [\mathbf{D}(\mathbf{w})]_{ii} \mathbf{K}(\mathcal{V}, i) \mathbf{K}(i, \mathcal{V}). \quad (14)$$

In the similar spirit as (3–5), we call this algorithm SSNCG, as it is a sub-sampled Newton method, where CG is used to find the Newton step.

Remark 1 *Since the focus of this work is on random features, we only compare RFN to the case that \mathcal{I} is chosen uniformly at random, i.e., the method would be a variant of uniform sub-sampled Newton (4). Nonuniform sampling methods give better approximations of the kernel at the cost of modifying the uniform sampling distribution. We refer the reader to Table 1 in (29) for various guarantees on the approximation quality via different sampling schemes.*

2.4 Comparison of Time Complexity

We compute the time complexity of finding the Newton step for four methods: Newton method, sub-sampled Newton method solved with CG exactly, sub-sampled Newton method solved with CG inexactly up to ε residual error, and random-feature based Newton method. The number of random features used by RFN is denoted by m . The size of the sub-sampled data points is $|\mathcal{I}|$, as discussed in Section 2.3. κ_{SSN} represents the upper bound of the condition number of the Hessian generated from sub-sampled data.

Table 1: Time Complexity per iteration.

Method	Complexity per iteration
Newton	$O(n^3)$
SSNCG(exact)	$O(\mathcal{I} n^2)$
SSNCG(inexact)	$O(\mathcal{I} ^2n + \mathcal{I} n\sqrt{\kappa_{SSN}} \log \varepsilon^{-1})$
RFN	$O(m^2n)$

3 Theoretical Results

In this section, we will study the convergence properties of our proposed method. In order to establish our results, we need to prove that the approximated Hessian mimics the spectrum of the original Hessian, which is described in Lemma 2. Notice that, throughout, for the presentation of our theoretical results we work with $\widehat{\mathbf{H}}(\mathbf{w})$ in (10) (rather than $\widehat{\mathbf{H}}_\mu(\mathbf{w})$).

3.1 Assumptions

Throughout the paper, we adhere to the following assumptions:

Assumption 1 (*Bounded Eigenvalues of Hessians*) *The objective function F is twice-differentiable and strongly convex and the smallest and the largest eigenvalues of the objective F is denoted as γ, L ($0 < \gamma, L < \infty$), i.e.,*

$$\gamma \mathbf{I} \leq \mathbf{H}(\mathbf{w}) \triangleq \nabla^2 F(\mathbf{w}) \leq L \mathbf{I}, \forall \mathbf{w} \in \mathbb{R}^n \quad (15)$$

and

$$\|\mathbf{D}(\mathbf{w})\| \leq \lambda_1 < \infty, \forall \mathbf{w} \in \mathbb{R}^n \quad (16)$$

For an approximated Hessian using m random features, we denote its maximum and minimum eigenvalues as $\lambda_{\max}(\widehat{\mathbf{H}}_m(\mathbf{w}))$ and $\lambda_{\min}(\widehat{\mathbf{H}}_m(\mathbf{w}))$ respectively.

Condition (16) is satisfied for common loss functions (e.g. quadratic loss and logistic loss). Furthermore, if we solve the risk minimization (2) with a positive definite kernel, the gram matrix \mathbf{K} would be positive definite and therefore Assumption 1 is satisfied. We also define the condition number κ of the Hessian matrix as follows:

$$\kappa \triangleq L/\gamma. \quad (17)$$

Assumption 2 (*Lipschitz Continuity of Hessian*) *The Hessian of the objective function F is Lipschitz continuous, i.e., there is a constant $M > 0$ such that*

$$\|\mathbf{H}(\mathbf{w}_1) - \mathbf{H}(\mathbf{w}_2)\| \leq M \|\mathbf{w}_1 - \mathbf{w}_2\|, \forall \mathbf{w}_1, \mathbf{w}_2 \in \mathbb{R}^n. \quad (18)$$

Assumption 2 is commonly used in the literature to establish super-linear convergence (see e.g., (3, 4, 24)).

We are now ready to show that the approximated Hessian is close enough to the original Hessian when large enough random features are sampled. We use $\tilde{\Omega}$ to hide the poly-logarithmic factors.

Lemma 2 (*The spectrum preserving inequality*) *Given any $0 < \epsilon \leq 1/2$ and $0 < \delta < 1$, if $m \geq \tilde{\Omega}(\max(\frac{\lambda_1 n^2}{\epsilon \zeta}, \frac{\lambda^2 n \|\mathbf{K}\|}{\epsilon^2 \zeta^2}))$, then we have that*

$$\Pr\left(\left\|\widehat{\mathbf{H}}(\mathbf{w}) - \mathbf{H}(\mathbf{w})\right\| \leq 4\epsilon\zeta\right) \geq 1 - \delta,$$

where $\zeta \leq \text{Tr}(\mathbf{K}) \|\mathbf{K}\| \lambda_1$.

From Lemma 2, we also know that with probability at least $(1 - \delta)$, we have

$$(1 - \epsilon\Psi)\gamma \leq \|\widehat{\mathbf{H}}(\mathbf{w})\| \leq (1 + \epsilon\Psi)L \quad (19)$$

where $\Psi = 4\zeta/\gamma$.

Notice that proving Lemma 2 with standard results in the literature of kernel approximation results in weaker guarantees. In particular, using ϵ -spectral approximation results (e.g., Theorem 1) or spectral norm errors for kernel approximation (e.g., Eq. (6.5.7) in (23)) give rise to $m = \Omega(\epsilon^{-2})$. However, Lemma 2 shows that the number of required features depends on the interplay of several parameters. In particular, when the regularization parameter λ is small enough, $m = \tilde{\Omega}(\epsilon^{-1})$ since we would be mainly concerned with approximating $\mathbf{KD}(\mathbf{w})\mathbf{K}$ in (3).

3.2 Global convergence

In this section, we will show the global convergence of our method with the spectral approximation inequality mentioned above. Recall that the update of the iterate is written as

$$\mathbf{w}_{t+1} = \mathbf{w}_t + \alpha_t \mathbf{p}_t, \quad (20)$$

where $\mathbf{p}_t = -[\widehat{\mathbf{H}}(\mathbf{w}_t)]^{-1}\nabla F(\mathbf{w}_t)$ and α_t is selected by Armijo-type line search such that

$$F(\mathbf{w}_t + \alpha_t \mathbf{p}_t) \leq F(\mathbf{w}_t) + \alpha_t \beta \mathbf{p}_t^T \nabla F(\mathbf{w}_t), \quad (21)$$

for some $\beta \in (0, 1)$. In what follows, we denote the minimizer of $F(\mathbf{w})$ by \mathbf{w}^* .

Theorem 3 (*Global convergence*) *By updating $\mathbf{w}_t \in \mathbb{R}^n$ using (20), with probability $1 - \delta$, we have*

$$F(\mathbf{w}_{t+1}) - F(\mathbf{w}^*) \leq (1 - \rho_t)(F(\mathbf{w}_t) - F(\mathbf{w}^*)), \quad (22)$$

where $\rho_t = 2\alpha_t\beta/((1 + \epsilon\Psi)\kappa)$. Moreover, the step size α_t is at least $2(1 - \beta)(1 - \epsilon\Psi)/\kappa$, where κ is defined in (17).

3.3 Local convergence

The classical Newton's method is appealing particularly for its local convergence property, resulting in quadratic rates for strongly convex and smooth problems. Even for weakly convex problems (the problems which are convex but not strongly convex), Newton's method has superlinear convergence with some modifications. In this section, we are going to discuss the local convergence behavior of our method. For the local case, we consider using a unit step size, i.e., $\alpha_t = 1$.

In the following lemma, we provide an error recursion for the update \mathbf{w}_t using Lemma 2.

Lemma 4 (*Error recursion*) *Let Assumptions 1-2 hold and set $m \geq \tilde{\Omega}(\max(\frac{\lambda_1 n^2}{\epsilon\zeta}, \frac{\lambda^2 n \|\mathbf{K}\|}{\epsilon^2 \zeta^2}))$. For the update equation (20) with $\alpha_t = 1$, with probability $1 - \delta$, we have*

$$\|\mathbf{w}_{t+1} - \mathbf{w}^*\| \leq \nu \|\mathbf{w}_t - \mathbf{w}^*\| + \eta \|\mathbf{w}_t - \mathbf{w}^*\|^2, \quad (23)$$

where $\nu = \frac{\epsilon\Psi}{1 - \epsilon\Psi}$ and $\eta = \frac{M}{2(1 - \epsilon\Psi)\gamma}$.

Theorem 5 (*Local linear convergence*) *Let Assumptions 1-2 hold. Consider any $0 < \nu < \rho < 1$. With $\epsilon \leq \frac{\nu}{\Psi(1 + \nu)}$, if*

$$\|\mathbf{w}_0 - \mathbf{w}^*\| \leq \frac{\rho - \nu}{\eta}, \quad (24)$$

where η is defined in Lemma 4, we have the linear convergence

$$\|\mathbf{w}_t - \mathbf{w}^*\| \leq \rho \|\mathbf{w}_{t-1} - \mathbf{w}^*\|, \quad t = 1, \dots, t_0 \quad (25)$$

with probability $(1 - t_0\delta)$.

Intuitively, if the precision of the Hessian approximation increases through iterations, it is expected that the algorithm can converge faster than the linear convergence. Here we show that if the Hessian approximation accuracy increases geometrically, the method can converge superlinearly.

Theorem 6 (*Local superlinearly convergence*) *Let the assumptions of theorem 5 hold. Defining the Hessian accuracy of each iteration as $\epsilon_t = \rho^t \epsilon$, $t = 0, 1, \dots, t_0$, if \mathbf{w}_0 fulfills equation (24) with ρ, ν and $\eta_0 \triangleq \frac{M}{2(1-\epsilon_0\Psi)\gamma}$, we have the superlinear convergence*

$$\|\mathbf{w}_t - \mathbf{w}^*\| \leq \rho^t \|\mathbf{w}_{t-1} - \mathbf{w}^*\|, \quad t = 1, \dots, t_0, \quad (26)$$

with probability $(1 - t_0\delta)$.

4 Numerical Experiments

We now provide numerical experiments to illustrate the performance of the random-feature based Newton method. We consider regularized kernel logistic regression

$$F(\mathbf{w}) = \frac{1}{n} \sum_{i=1}^n \log(1 + \exp(-y_i \sum_{j=1}^n k(\mathbf{x}_i, \mathbf{x}_j) w_j)) + \lambda \|\mathbf{w}\|_{\mathbf{K}}^2,$$

where $k(\mathbf{x}, \mathbf{x}') = e^{-\frac{\sigma^2 \|\mathbf{x} - \mathbf{x}'\|^2}{2}}$ is chosen to be a Gaussian kernel, and $\|\mathbf{w}\|_{\mathbf{K}}^2 = \mathbf{w}^T \mathbf{K} \mathbf{w}$ is the norm with respect to the gram matrix.

Benchmark algorithms: We compare RFN (as described in Algorithm 1) with three other benchmarks, listed below:

1. **Newton:** The exact Newton method $\mathbf{w}_{t+1} = \mathbf{w}_t + \alpha_t \mathbf{p}_t$, where \mathbf{p}_t is the exact solution of the linear system $\mathbf{H}(\mathbf{w}_t) \mathbf{p}_t = -\nabla F(\mathbf{w}_t)$.

2. **SSNCG:** The sub-sampled Newton method with conjugate gradient update $\mathbf{w}_{t+1} = \mathbf{w}_t + \alpha_t \mathbf{p}_t$, where \mathbf{p}_t is computed by solving the linear system $\widehat{\mathbf{H}}_{\text{SSN}}(\mathbf{w}_t) \mathbf{p}_t = -\nabla F(\mathbf{w}_t)$ up to a high precision by the CG method. The approximated Hessian $\widehat{\mathbf{H}}_{\text{SSN}}(\mathbf{w}_t)$ is generated as described in Section 2.3 (see (13)-(14)), i.e.,

$$\widehat{\mathbf{H}}_{\text{SSN}}(\mathbf{w}) = \sum_{i \in \mathcal{I}} [\mathbf{D}(\mathbf{w})]_{ii} \mathbf{K}(\mathcal{V}, i) \mathbf{K}(i, \mathcal{V}) + \lambda \mathbf{K}(\mathcal{V}, \mathcal{I}) \mathbf{K}(\mathcal{I}, \mathcal{I})^\dagger \mathbf{K}(\mathcal{I}, \mathcal{V}),$$

where \mathcal{I} is random subset. We also add a regularization term $\mu \mathbf{I}$ to above to avoid singularity.

3. **L-BFGS:** Limited-memory BFGS which approximates the Newton direction using the first order information. Here, we implement BFGS using the history of the past 50 updates of \mathbf{w}_t and $\nabla F(\mathbf{w}_t)$.

For all these methods, the step size α_t is determined by Armijo backtracking line search, and the full gradient $\nabla F(\mathbf{w}_t)$ is used. For SSNCG, the linear system is solved approximately to achieve 10^{-6} relative error.

Hyper-parameters of the empirical risk: There are two hyper-parameters in the regularized kernel logistic regression: σ and λ . λ determines the rate by which we impose the RKHS norm as a penalty function. When λ is small, the model fits the training data. On the other hand, σ determines the kernel characteristics. As it grows larger, the gram matrix gets closer to a full-rank matrix, and this in turns increases the number of random features (or the number of sub-sampled data points) that randomized optimization methods (i.e., SSNCG and RFN) require to achieve good approximations of the original Hessian.

Hyper-parameter of backtracking line search: We use a simple grid search to optimize the parameters for Newton and L-BFGS. However, due to the randomness of the approximated Hessian for randomized methods, we perform the line search adaptively for both SSNCG and RFN. For each iteration, the initial step size of backtracking is set as twice of the step size chosen in the previous iteration. This allows the

Table 2: Descriptions of datasets used in the experiments.

Data set	Data points	Features	References
Coverttype	581012	54	(30)
Cod-RNA	59535	8	(31)

algorithms to avoid staying in the search loop for long.

Datasets: We apply all of the methods on two datasets from the UCI Machine Learning Repository (Table 2). For each dataset, we randomly select 5000 data points for training to run the optimization.

1. **Coverttype:** For this data set, the hyper-parameters of the objective function are set as follows: $\sigma = 0.5, \lambda = 10^{-5}$. For backtracking, we have two setups for randomized methods and non-randomized methods, respectively. For Newton and L-BFGS, $\alpha = 0.3, \beta = 0.5$ and the initial step size of backtracking is always set as 1. For SSNCG and RFN, $\alpha = 0.3, \beta = 0.2$ and the initial step size of backtracking is set as the inverse of squared Newton decrement.
2. **Cod-RNA:** For this data set, the hyper-parameters are set as follows: $\sigma = 2; \lambda = 10^{-5}; \alpha = 0.3, \beta = 0.5$ for Newton and LBFGS and $\alpha = 0.3, \beta = 0.25$ for SSNCG and RFN.

About the number of random features for RFN (m) and the number of sub-sampled data points for SSNCG ($|\mathcal{I}|$), we set the ratio as 10% of the training data for both data sets. To prevent the approximated Hessians of RFN and SSNCG from being singular, a regularizer term $\mu \mathbf{I}$ is added with $\mu = 10^{-4}$.

Performance: We record the loss value and the time cost of each iteration for all methods. The time cost includes the time of finding the Newton direction (computing the Hessian and solving the linear system) and determining the step size. The run time is obtained on a desktop with an 8-core, 3.00 Intel Core i7-9700 CPU and 15.5G of RAM (2666Mhz). The initial point \mathbf{w}_0 is generated from a standard Gaussian distribution. We run the experiment 40 times and calculate the standard errors for both loss value and time cost.

Based on Fig. 1, we see that the two randomized methods outperform the classical Newton method with time cost benefits from a small number of random features (or sub-sampled data points). RFN also out-

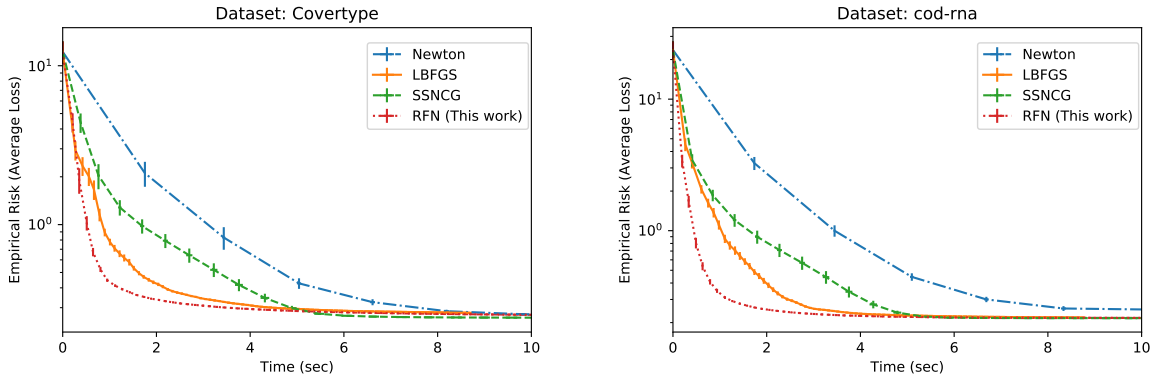


Figure 1: The plot of empirical risk (training error) vs. time cost shows that RFN enjoys a faster decay rate compared to other methods.

performs L-BFGS, which approximates the newton direction using the first order information.

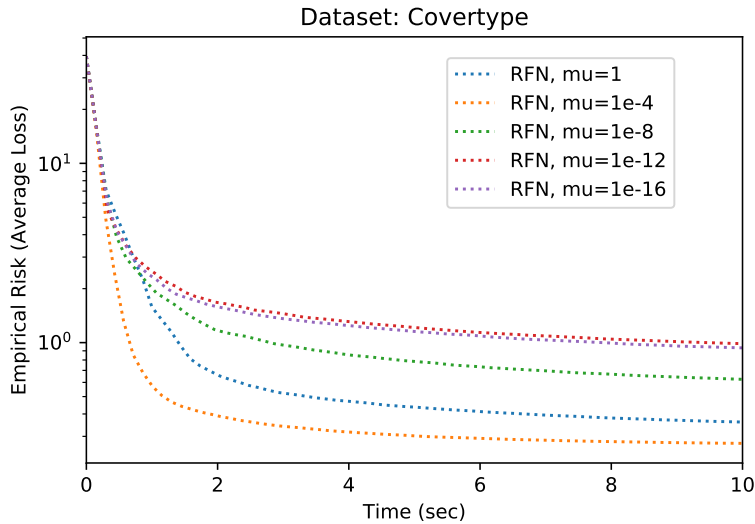


Figure 2: Sensitivity of empirical risk to μ .

Sensitivity to μ : To evaluate the sensitivity of RFN to the value of μ , we run the experiment of Covertypes data set with the same hyper parameter setting except μ . For this experiment, we choose $\mu \in \{1, 10^{-4}, 10^{-8}, 10^{-12}, 10^{-16}\}$. For each μ , we run the simulation 10 times and obtain the averaged loss. Based on Fig. 2, we find out that when μ is too small, the convergence rate is adversely affected

by the singularity of the approximated Hessian. On the other hand, if the value of μ is too large, the regularizer dominates and RFN tends to behave like gradient descent. There is, however, a sweet spot in between where RFN performs best. Of course, this sweet spot entirely depends on the kernel choice and dataset, and it would be different across different problem environments.

Performance for various numbers of features m : Another factor affecting the convergence performance of RFN is the number of random features. To see this property, we run the experiment on Covertype data set with the same hyper-parameter set up except that μ is fixed as 10^{-6} and the ratio (m/n) ranges in the set 10%, 40%, 70%. Figs. 3- 4 verify that with more random features, the convergence is faster in terms of iterations, but this comes at the cost of increased run time. Using more random features improves the Hessian approximation, but it also increases the size of matrix \mathbf{C} in (12), which needs to be inverted.

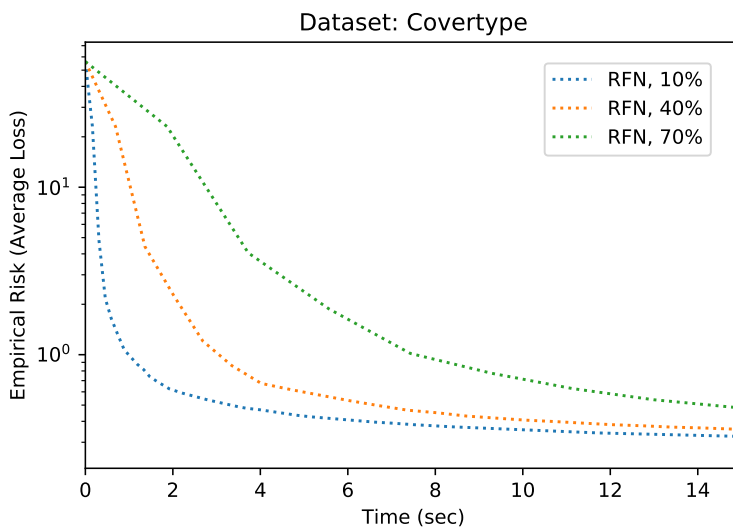


Figure 3: Empirical risk vs. time cost for different ratios of m/n .

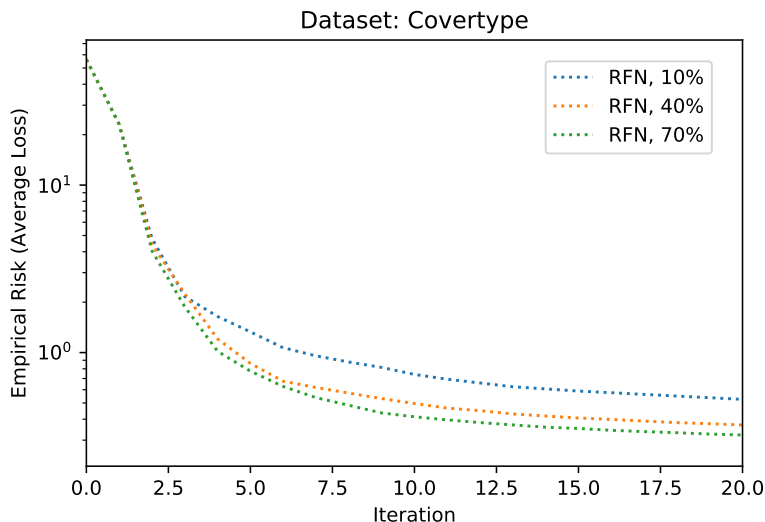


Figure 4: Empirical risk vs. iterations for different ratios of m/n .

5 Conclusion

In this paper, we propose a random-feature based Newton method (RFN) for risk minimization over RKHS. We draw explicit connections between the Hessian and the gram matrix and observe that subsampled Newton methods are not directly applicable to this optimization problem. Then, we show that the Newton method can be expedited by applying kernel approximation techniques. From the theoretical point of view, we prove that the approximate Hessian is close to the original Hessian in terms of spectral norm when enough random features are sampled, which in turn ensures the local and global convergence with high probability. From the practical point of view, we apply RFN to two real-world data sets, compare it with three other benchmarks, and show that RFN enjoys a faster run time under certain conditions.

References and Notes

1. L. Bottou, F. E. Curtis, and J. Nocedal, “Optimization methods for large-scale machine learning,” *Siam Review*, vol. 60, no. 2, pp. 223–311, 2018.

2. Y. Nesterov, "Introductory lectures on convex programming volume i: Basic course," *Lecture notes*, vol. 3, no. 4, p. 5, 1998.
3. R. Bollapragada, R. H. Byrd, and J. Nocedal, "Exact and inexact subsampled newton methods for optimization," *IMA Journal of Numerical Analysis*, vol. 39, no. 2, pp. 545–578, 2018.
4. F. Roosta-Khorasani and M. W. Mahoney, "Sub-sampled newton methods," *Mathematical Programming*, vol. 174, no. 1-2, pp. 293–326, 2019.
5. P. Xu, J. Yang, F. Roosta-Khorasani, C. Ré, and M. W. Mahoney, "Sub-sampled newton methods with non-uniform sampling," in *Advances in Neural Information Processing Systems*, 2016, pp. 3000–3008.
6. M. Pilanci and M. J. Wainwright, "Newton sketch: A near linear-time optimization algorithm with linear-quadratic convergence," *SIAM Journal on Optimization*, vol. 27, no. 1, pp. 205–245, 2017.
7. C. G. Broyden, "The convergence of a class of double-rank minimization algorithms: 2. the new algorithm," *IMA journal of applied mathematics*, vol. 6, no. 3, pp. 222–231, 1970.
8. R. Fletcher, "A new approach to variable metric algorithms," *The computer journal*, vol. 13, no. 3, pp. 317–322, 1970.
9. D. Goldfarb, "A family of variable-metric methods derived by variational means," *Mathematics of computation*, vol. 24, no. 109, pp. 23–26, 1970.
10. D. F. Shanno, "Conditioning of quasi-newton methods for function minimization," *Mathematics of computation*, vol. 24, no. 111, pp. 647–656, 1970.
11. N. N. Schraudolph, J. Yu, and S. Günter, "A stochastic quasi-newton method for online convex optimization," in *Artificial intelligence and statistics*, 2007, pp. 436–443.

12. A. Mokhtari and A. Ribeiro, “Res: Regularized stochastic bfgs algorithm,” *IEEE Transactions on Signal Processing*, vol. 62, no. 23, pp. 6089–6104, 2014.
13. R. H. Byrd, S. L. Hansen, J. Nocedal, and Y. Singer, “A stochastic quasi-newton method for large-scale optimization,” *SIAM Journal on Optimization*, vol. 26, no. 2, pp. 1008–1031, 2016.
14. J. Shawe-Taylor, N. Cristianini *et al.*, *Kernel methods for pattern analysis*. Cambridge university press, 2004.
15. A. Rahimi and B. Recht, “Random features for large-scale kernel machines,” in *Advances in neural information processing systems*, 2008, pp. 1177–1184.
16. P. Moritz, R. Nishihara, and M. Jordan, “A linearly-convergent stochastic l-bfgs algorithm,” in *Artificial Intelligence and Statistics*, 2016, pp. 249–258.
17. R. H. Byrd, G. M. Chin, W. Neveitt, and J. Nocedal, “On the use of stochastic hessian information in optimization methods for machine learning,” *SIAM Journal on Optimization*, vol. 21, no. 3, pp. 977–995, 2011.
18. R. H. Byrd, G. M. Chin, J. Nocedal, and Y. Wu, “Sample size selection in optimization methods for machine learning,” *Mathematical programming*, vol. 134, no. 1, pp. 127–155, 2012.
19. C.-C. Wang, C.-H. Huang, and C.-J. Lin, “Subsampled hessian newton methods for supervised learning,” *Neural computation*, vol. 27, no. 8, pp. 1766–1795, 2015.
20. J. Martens, “Deep learning via hessian-free optimization.” in *ICML*, vol. 27, 2010, pp. 735–742.
21. M. A. Erdogdu and A. Montanari, “Convergence rates of sub-sampled newton methods,” in *NIPS*, 2015.
22. J. A. Tropp and S. J. Wright, “Computational methods for sparse solution of linear inverse problems,” *Proceedings of the IEEE*, vol. 98, no. 6, pp. 948–958, 2010.

23. J. A. Tropp *et al.*, “An introduction to matrix concentration inequalities,” *Foundations and Trends® in Machine Learning*, vol. 8, no. 1-2, pp. 1–230, 2015.
24. N. Agarwal, B. Bullins, and E. Hazan, “Second-order stochastic optimization for machine learning in linear time,” *The Journal of Machine Learning Research*, vol. 18, no. 1, pp. 4148–4187, 2017.
25. M. Mutny, “Stochastic second-order optimization via von neumann series,” *arXiv preprint arXiv:1612.04694*, 2016.
26. P. Kar and H. Karnick, “Random feature maps for dot product kernels,” in *International conference on Artificial Intelligence and Statistics*, 2012, pp. 583–591.
27. J. Yang, V. Sindhwani, Q. Fan, H. Avron, and M. W. Mahoney, “Random laplace feature maps for semigroup kernels on histograms,” in *Proceedings of the IEEE Conference on Computer Vision and Pattern Recognition*, 2014, pp. 971–978.
28. H. Avron, M. Kapralov, C. Musco, C. Musco, A. Velingker, and A. Zandieh, “Random fourier features for kernel ridge regression: Approximation bounds and statistical guarantees,” in *Proceedings of the 34th International Conference on Machine Learning-Volume 70*, 2017, pp. 253–262.
29. A. Gittens and M. W. Mahoney, “Revisiting the nystrom method for improved large-scale machine learning,” *The Journal of Machine Learning Research*, vol. 17, no. 1, pp. 3977–4041, 2016.
30. J. A. Blackard and D. J. Dean, “Comparative accuracies of artificial neural networks and discriminant analysis in predicting forest cover types from cartographic variables,” *Computers and electronics in agriculture*, vol. 24, no. 3, pp. 131–151, 1999.
31. A. V. Uzilov, J. M. Keegan, and D. H. Mathews, “Detection of non-coding rnas on the basis of predicted secondary structure formation free energy change,” *BMC bioinformatics*, vol. 7, no. 1, p. 173, 2006.

6 Supplementary Material

We make use of the matrix Bernstein inequality (23) for the proof of Lemma 2, but we adopt the version presented in (28).

Lemma 7 (*Matrix Concentration Inequality*) Let \mathbf{B} be a fixed $d_1 \times d_2$ matrix. Construct a $d_1 \times d_2$ random matrix \mathbf{R} that satisfies

$$\mathbb{E}[\mathbf{R}] = \mathbf{B} \quad \text{and} \quad \|\mathbf{R}\|_2 \leq U$$

Let \mathbf{M}_1 and \mathbf{M}_2 be semidefinite upper bounds for the expected squares:

$$\mathbb{E}[\mathbf{R}\mathbf{R}^*] \preceq \mathbf{M}_1 \quad \text{and} \quad \mathbb{E}[\mathbf{R}^*\mathbf{R}] \preceq \mathbf{M}_2$$

Define the quantities $c = \max(\|\mathbf{M}_1\|_2, \|\mathbf{M}_2\|_2)$ and $d = (\text{Tr}(\mathbf{M}_1) + \text{Tr}(\mathbf{M}_2))/c$. Form the matrix sampling estimator

$$\bar{\mathbf{R}}_n = \frac{1}{n} \sum_{k=1}^n \mathbf{R}_k,$$

where each \mathbf{R}_k is an independent copy of \mathbf{R} . Then, for all $t \geq \sqrt{c/n} + 2U/3n$,

$$\Pr(\|\bar{\mathbf{R}}_n - \mathbf{B}\|_2 \geq t) \leq 4d \exp\left(\frac{-nt^2/2}{c + 2Ut/3}\right).$$

6.1 Proof of Lemma 2

Our goal is to find the probability bound for the norm of the difference between the approximated Hessian $\hat{\mathbf{H}}$ and the original Hessian \mathbf{H} :

$$\begin{aligned} & \left\| \hat{\mathbf{H}} - \mathbf{H} \right\| \\ &= \left\| (\mathbf{Z}\mathbf{Z}^T \mathbf{D}\mathbf{Z}\mathbf{Z}^T + \lambda\mathbf{Z}\mathbf{Z}^T) - (\mathbf{K}\mathbf{D}\mathbf{K} + \lambda\mathbf{K}) \right\| \end{aligned}$$

Since $\|\mathbf{A} + \mathbf{B}\| \leq \|\mathbf{A}\| + \|\mathbf{B}\|$, we would find the bounds for $\|\mathbf{Z}\mathbf{Z}^T \mathbf{D}\mathbf{Z}\mathbf{Z}^T - \mathbf{K}\mathbf{D}\mathbf{K}\|$ and $\|\lambda\mathbf{Z}\mathbf{Z}^T - \lambda\mathbf{K}\|$ in **Part 1** and **Part 2** respectively.

Part 1:

First we denote $\mathbf{z}(\omega_i)$ as \mathbf{z}_i and $\widehat{\mathbf{K}}\mathbf{D}\widehat{\mathbf{K}}$ can be written as $\frac{1}{m^2} \sum_{i=1}^m \sum_{j=1}^m (\mathbf{z}_i \mathbf{z}_i^T \mathbf{D} \mathbf{z}_j \mathbf{z}_j^T)$. For this summation term, we actually find out that $\mathbb{E}[\mathbf{z}_i \mathbf{z}_i^T \mathbf{D} \mathbf{z}_j \mathbf{z}_j^T] = \mathbf{K} \mathbf{D} \mathbf{K}$ as $i \neq j$. Based on this fact, we apply lemma 7 as the following:

Let $\mathbf{R} = \mathbf{z}_i \mathbf{z}_i^T \mathbf{D} \mathbf{z}_j \mathbf{z}_j^T$. Given that fact that $\mathbf{z}_i^T \mathbf{z}_j \leq n$ and $\|\mathbf{z}_i \mathbf{z}_j^T\| \leq n \quad \forall i, j$, we know that

$$\|\mathbf{R}\| \leq \lambda_1 n^2 := U.$$

Since

$$\begin{aligned} \mathbf{R} \mathbf{R}^* &= \mathbf{z}_i \mathbf{z}_i^T \mathbf{D} \mathbf{z}_j \mathbf{z}_j^T \mathbf{z}_j \mathbf{z}_j^T \mathbf{D} \mathbf{z}_i \mathbf{z}_i^T \\ &\leq \lambda_1^2 n^2 \text{Tr}(\mathbf{z}_j \mathbf{z}_j^T) \mathbf{z}_i \mathbf{z}_i^T, \end{aligned}$$

we get

$$\mathbb{E}[\mathbf{R} \mathbf{R}^*] \leq \lambda_1^2 n^2 \text{Tr}(\mathbf{K}) \mathbf{K} := \mathbf{M}_1 (\mathbf{M}_2)$$

and

$$\begin{aligned} c &= \lambda_1^2 n^2 \text{Tr}(\mathbf{K}) \|\mathbf{K}\| \\ d &= \frac{2 \text{Tr}(\mathbf{M}_1)}{c} = \frac{2 \text{Tr}(\mathbf{K})}{\|\mathbf{K}\|}. \end{aligned}$$

With the above quantities, based on lemma 7, we get

$$\begin{aligned} &\Pr\left(\left\|\left(\frac{1}{m^2 - m} \sum_{i \neq j} \mathbf{z}_i \mathbf{z}_i^T \mathbf{D} \mathbf{z}_j \mathbf{z}_j^T\right) - \mathbf{K} \mathbf{D} \mathbf{K}\right\| \geq \epsilon \zeta\right) \\ &\leq 4d \exp\left(\frac{-(m^2 - m) \epsilon^2 \zeta^2 / 2}{\lambda_1^2 n^2 \text{Tr}(\mathbf{K}) \|\mathbf{K}\| + \frac{2}{3} \lambda_1 n^2 \epsilon \zeta}\right) \end{aligned}$$

Assume

$$4d \exp\left(\frac{-(m^2 - m) \epsilon^2 \zeta^2 / 2}{\lambda_1^2 n^2 \text{Tr}(\mathbf{K}) \|\mathbf{K}\| + \frac{2}{3} \lambda_1 n^2 \epsilon \zeta}\right) \leq \delta,$$

we have

$$\log\left(\frac{4d}{\delta}\right) \leq \left(\frac{(m^2 - m) \epsilon^2 \zeta^2 / 2}{\lambda_1^2 n^2 \text{Tr}(\mathbf{K}) \|\mathbf{K}\| + \frac{2}{3} \lambda_1 n^2 \epsilon \zeta}\right).$$

Assume $m \geq 2$, then

$$m^2 - m \geq \frac{1}{2}m^2 \geq \tilde{\Omega}\left(\frac{\lambda_1^2 n^2 \text{Tr}(\mathbf{K}) \|\mathbf{K}\| + \frac{2}{3}\lambda_1 n^2 \epsilon \zeta}{\epsilon^2 \zeta^2}\right)$$

Therefore, with

$$m \geq \tilde{\Omega}\left(\frac{\sqrt{\lambda_1^2 n^2 \text{Tr}(\mathbf{K}) \|\mathbf{K}\| + \frac{2}{3}\lambda_1 n^2 \epsilon \zeta}}{\epsilon \zeta}\right), \quad (27)$$

we have

$$\Pr\left(\left\|\left(\frac{1}{m^2 - m} \sum_{i \neq j} \mathbf{z}_i \mathbf{z}_i^T \mathbf{D} \mathbf{z}_j \mathbf{z}_j^T\right) - \mathbf{K} \mathbf{D} \mathbf{K}\right\| < \epsilon \zeta\right) > (1 - \delta)$$

Now go back to $\|\mathbf{Z} \mathbf{Z}^T \mathbf{D} \mathbf{Z} \mathbf{Z}^T - \mathbf{K} \mathbf{D} \mathbf{K}\|$, which can be written as

$$\begin{aligned} & \left\| \frac{1}{m^2} \sum_{i \neq j} \mathbf{z}_i \mathbf{z}_i^T \mathbf{D} \mathbf{z}_j \mathbf{z}_j^T + \frac{1}{m^2} \sum_{i=j} \mathbf{z}_i \mathbf{z}_i^T \mathbf{D} \mathbf{z}_j \mathbf{z}_j^T - \mathbf{K} \mathbf{D} \mathbf{K} \right\| \\ & \leq \frac{m^2 - m}{m^2} \left\| \frac{1}{m^2 - m} \sum_{i \neq j} \mathbf{z}_i \mathbf{z}_i^T \mathbf{D} \mathbf{z}_j \mathbf{z}_j^T - \mathbf{K} \mathbf{D} \mathbf{K} \right\| \\ & \quad + \frac{1}{m^2} \left\| \sum_{i=j} \mathbf{z}_i \mathbf{z}_i^T \mathbf{D} \mathbf{z}_j \mathbf{z}_j^T \right\| + \frac{1}{m} \|\mathbf{K} \mathbf{D} \mathbf{K}\|. \end{aligned}$$

The first norm term, based on lemma 7, has been shown that it is bounded by $\epsilon \zeta$ if equation (27) holds.

For the second and third norm terms, knowing that $\|\mathbf{z}_i \mathbf{z}_j^T\| \leq n \quad \forall i, j$ and $\|\mathbf{K}\| \leq n$, we get

$$\frac{1}{m^2} \left\| \sum_{i=j} \mathbf{z}_i \mathbf{z}_i^T \mathbf{D} \mathbf{z}_j \mathbf{z}_j^T \right\| \leq \frac{1}{m^2} m \lambda_1 n^2 = \frac{1}{m} \lambda_1 n^2$$

and

$$\frac{1}{m} \|\mathbf{K} \mathbf{D} \mathbf{K}\| \leq \frac{1}{m} \lambda_1 n^2.$$

If $m \geq \frac{\lambda_1 n^2}{\epsilon \zeta}$, then the second and third norm terms are also bounded by $\epsilon \zeta$.

Therefore, if

$$m \geq \tilde{\Omega}\left(\max\left(\frac{\sqrt{\lambda_1^2 n^2 \text{Tr}(\mathbf{K}) \|\mathbf{K}\| + \frac{2}{3}\lambda_1 n^2 \epsilon \zeta}}{\epsilon \zeta}, \frac{\lambda_1 n^2}{\epsilon \zeta}\right)\right),$$

then $\left\| \widehat{\mathbf{K}}\widehat{\mathbf{D}}\widehat{\mathbf{K}} - \mathbf{K}\mathbf{D}\mathbf{K} \right\|$ is bounded by $\epsilon\zeta$ with probability at least $(1 - \delta)$.

Now we further assume that $\zeta \leq \lambda_1 \text{Tr}(\mathbf{K}) \|\mathbf{K}\|$ and $\epsilon \in (0, 1/2]$, then the lower bound on m becomes

$$m \geq \tilde{\Omega}\left(\max\left(\frac{\sqrt{\lambda_1^2 n^2 \text{Tr}(\mathbf{K}) \|\mathbf{K}\|}}{\epsilon\zeta}, \frac{\lambda_1 n^2}{\epsilon\zeta}\right)\right).$$

Since both $\text{Tr}(\mathbf{K})$ and $\|\mathbf{K}\|$ are upper bounded by n , the above inequality becomes

$$m \geq \frac{\lambda_1 n^2}{\epsilon\zeta}$$

Part 2:

For $\left\| \lambda \mathbf{Z}\mathbf{Z}^T - \lambda \mathbf{K} \right\|$, which can be written as $\left\| \frac{\lambda}{m} \sum_{i=1}^m \mathbf{z}_i \mathbf{z}_i^T - \lambda \mathbf{K} \right\|$, we notice that $\mathbb{E}[\mathbf{z}_i \mathbf{z}_i^T] = \mathbf{K}$.

Based on lemma 7, we have the following derivation:

Let $\mathbf{R} = \lambda \mathbf{z}_i \mathbf{z}_i^T$. We have $\|\mathbf{R}\| \leq \lambda n := U$.

Since

$$\begin{aligned} \mathbf{R}\mathbf{R}^* &= \lambda^2 \mathbf{z}_i \mathbf{z}_i^T \mathbf{z}_i \mathbf{z}_i^T \\ &\leq \lambda^2 n \mathbf{z}_i \mathbf{z}_i^T, \end{aligned}$$

we get

$$\mathbb{E}[\mathbf{R}\mathbf{R}^*] \leq \lambda^2 n \mathbf{K} := \mathbf{M}_1 (\mathbf{M}_2)$$

and

$$\begin{aligned} c &= \lambda^2 n \|\mathbf{K}\| \\ d &= \frac{2\text{Tr}(\mathbf{M}_1)}{c} = \frac{2\text{Tr}(\mathbf{K})}{\|\mathbf{K}\|}. \end{aligned}$$

With the above quantities, based on lemma 7, we get

$$\begin{aligned} &\Pr\left(\left\| \frac{\lambda}{m} \sum_i \mathbf{z}_i \mathbf{z}_i^T - \lambda \mathbf{K} \right\| \geq \epsilon\zeta\right) \\ &\leq 4d \exp \frac{-m\epsilon^2\zeta^2/2}{\lambda^2 n \|\mathbf{K}\| + \frac{2}{3}\lambda n \epsilon\zeta} \end{aligned}$$

Assume

$$4d \exp \frac{-m\epsilon^2\zeta^2/2}{\lambda^2 n \|\mathbf{K}\| + \frac{2}{3}\lambda n \epsilon \zeta} \leq \delta$$

we have

$$\log\left(\frac{4d}{\delta}\right) \leq \left(\frac{m\epsilon^2\zeta^2/2}{\lambda^2 n \|\mathbf{K}\| + \frac{2}{3}\lambda n \epsilon \zeta}\right).$$

Therefore, with

$$m \geq \tilde{\Omega}\left(\frac{\lambda^2 n \|\mathbf{K}\| + \frac{2}{3}\lambda n \epsilon \zeta}{\epsilon^2 \zeta^2}\right),$$

we have

$$\Pr\left(\left\|\frac{\lambda}{m} \sum_i \mathbf{z}_i \mathbf{z}_i^T - \lambda \mathbf{K}\right\| < \epsilon \zeta\right) > (1 - \delta)$$

Now by combining the results from **Part 1** and **Part 2**, we have that if

$$m \geq \tilde{\Omega}\left(\max\left(\frac{\lambda_1 n^2}{\epsilon \zeta}, \frac{\lambda^2 n \|\mathbf{K}\|}{\epsilon^2 \zeta^2}, \frac{\lambda n}{\epsilon \zeta}\right)\right),$$

where the last two terms come from **Part 2**, $\|\widehat{\mathbf{H}} - \mathbf{H}\|$ is bounded by $4\epsilon\zeta$ with probability at least $(1 - \delta)$.

Typically, λ is a small constant less than n , so $\frac{\lambda n}{\epsilon \zeta}$ can be negligible as compared to $\frac{\lambda_1 n^2}{\epsilon \zeta}$. Based on this,

the above inequality becomes

$$m \geq \tilde{\Omega}\left(\max\left(\frac{\lambda_1 n^2}{\epsilon \zeta}, \frac{\lambda^2 n \|\mathbf{K}\|}{\epsilon^2 \zeta^2}\right)\right).$$

For our theoretical results, we mainly follow the structure of (4) and interested readers can find out more discussion there. The difference here is that a different Hessian approximation inequality is applied for our specific kernel problem, and we include the proofs for the sake of completeness.

6.2 Proof of Theorem 3

Denotes the minimum eigenvalue of $\widehat{\mathbf{H}}(\mathbf{w}_t)$ as $\lambda_{\min}(\widehat{\mathbf{H}}(\mathbf{w}_t))$. Since $\mathbf{p}_t^T \widehat{\mathbf{H}}(\mathbf{w}_t) \mathbf{p}_t \geq \lambda_{\min}(\widehat{\mathbf{H}}(\mathbf{w}_t)) \|\mathbf{p}_t\|^2$,

by Lemma 2, we have that

$$\mathbf{p}_t^T \widehat{\mathbf{H}}(\mathbf{w}_t) \mathbf{p}_t \geq (1 - \epsilon \Psi) \gamma \|\mathbf{p}_t\|^2.$$

For any $\alpha > 0$, define $\mathbf{w}_\alpha = \mathbf{w}_t + \alpha \mathbf{p}_t$. With the strong convexity of the objective function F , we have

$$\begin{aligned} & F(\mathbf{w}_\alpha) - F(\mathbf{w}_t) \\ & \leq (\mathbf{w}_\alpha - \mathbf{w}_t)^T \nabla F(\mathbf{w}_t) + \frac{L}{2} \|\mathbf{w}_\alpha - \mathbf{w}_t\|^2 \\ & = \alpha \mathbf{p}_t^T \nabla F(\mathbf{w}_t) + \frac{\alpha^2 L}{2} \|\mathbf{p}_t\|^2 \end{aligned}$$

To pass the Armijo line-search, we need the α which makes the following inequality hold

$$\alpha \mathbf{p}_t^T \nabla F(\mathbf{w}_t) + \frac{\alpha^2 L}{2} \|\mathbf{p}_t\|^2 \leq \alpha \beta \mathbf{p}_t^T \nabla F(\mathbf{w}_t).$$

Knowing that $\mathbf{p}_t^T \nabla F(\mathbf{w}_t) = -\mathbf{p}_t^T \widehat{\mathbf{H}}(\mathbf{w}_t) \mathbf{p}_t$, the above inequality can be written as

$$\alpha L \|\mathbf{p}_t\|^2 \leq 2(1 - \beta) \mathbf{p}_t^T \widehat{\mathbf{H}}(\mathbf{w}_t) \mathbf{p}_t.$$

Therefore, if $\alpha \leq 2(1 - \beta)(1 - \epsilon\Psi)/\kappa$ (given that $\mathbf{p}_t^T \widehat{\mathbf{H}}(\mathbf{w}_t) \mathbf{p}_t \geq (1 - \epsilon\Psi)\gamma \|\mathbf{p}_t\|^2$), it suffices to pass the Armijo rule and this quantity is iteration-independent and can be the least step size for each iteration.

Now suppose $\mathbf{w}_{t+1} = \mathbf{w}_t + \alpha_t^T \mathbf{p}_t$, based on (21), we have

$$\begin{aligned} F(\mathbf{w}_{t+1}) & \leq F(\mathbf{w}_t) + \alpha_t \beta \mathbf{p}_t^T \nabla F(\mathbf{w}_t) \\ & = F(\mathbf{w}_t) - \alpha_t \beta \nabla F(\mathbf{w}_t)^T [\widehat{\mathbf{H}}(\mathbf{w}_t)]^{-1} \nabla F(\mathbf{w}_t) \\ & \leq F(\mathbf{w}_t) - \alpha_t \beta \frac{\|\nabla F(\mathbf{w}_t)\|^2}{(1 + \epsilon\Psi)L} \end{aligned}$$

By subtracting $F(\mathbf{w}^*)$ from both sides and noting that $F(\mathbf{w}_t) - F(\mathbf{w}^*) \leq \frac{\|\nabla F(\mathbf{w}_t)\|^2}{2\gamma}$ due to the strong convexity of F , the result is proved.

Lemma 8 (*Error recursion*) *Let Assumption 2 hold and assume that $\alpha_t = 1$ and $\widehat{\mathbf{H}}(\mathbf{w})$ is positive definite, we have*

$$\|\mathbf{w}_{t+1} - \mathbf{w}^*\| \leq \nu \|\mathbf{w}_t - \mathbf{w}^*\| + \eta \|\mathbf{w}_t - \mathbf{w}^*\|^2,$$

where $\eta \triangleq \frac{M}{2\lambda_{\min}(\widehat{\mathbf{H}}(\mathbf{w}_t))}$ and $\nu \triangleq \frac{\|\widehat{\mathbf{H}}(\mathbf{w}_t) - \mathbf{H}(\mathbf{w}_t)\|}{\lambda_{\min}(\widehat{\mathbf{H}}(\mathbf{w}_t))}$.

6.3 Proof of Lemma 8

Define $\Delta_t \triangleq \mathbf{w}_t - \mathbf{w}^*$. Since $\mathbf{w}_{t+1} = \mathbf{w}_t - \widehat{\mathbf{H}}(\mathbf{w}_t)^{-1} \nabla F(\mathbf{w}_t)$, \mathbf{w}_{t+1} is the optimal solution of the second order approximation equation:

$$\begin{aligned} N(\mathbf{w}) &= F(\mathbf{w}_t) + (\mathbf{w} - \mathbf{w}_t)^T \nabla F(\mathbf{w}_t) \\ &\quad + \frac{1}{2} (\mathbf{w} - \mathbf{w}_t)^T \widehat{\mathbf{H}}(\mathbf{w}_t) (\mathbf{w} - \mathbf{w}_t). \end{aligned}$$

Based on that, for any $\mathbf{w} \in \mathbb{R}^n$, we have

$$\begin{aligned} 0 &\leq (\mathbf{w} - \mathbf{w}_{t+1})^T \nabla N(\mathbf{w}_{t+1}) \\ &= (\mathbf{w} - \mathbf{w}_{t+1})^T \nabla F(\mathbf{w}_t) + (\mathbf{w} - \mathbf{w}_{t+1})^T \widehat{\mathbf{H}}(\mathbf{w}_t) (\mathbf{w}_{t+1} - \mathbf{w}_t). \end{aligned}$$

By setting $\mathbf{w} = \mathbf{w}^*$ and noting that $\mathbf{w}_{t+1} - \mathbf{w}_t = \Delta_{t+1} - \Delta_t$, we have

$$\Delta_{t+1}^T \widehat{\mathbf{H}}(\mathbf{w}_t) \Delta_{t+1} \leq \Delta_{t+1}^T \widehat{\mathbf{H}}(\mathbf{w}_t) \Delta_t - \Delta_{t+1}^T \nabla F(\mathbf{w}_t).$$

The optimality of \mathbf{w}^* on F gives that $\nabla F(\mathbf{w}^*)^T (\mathbf{w}_{t+1} - \mathbf{w}^*) \geq 0$, which is added to the right hand side of the above inequality and get $\Delta_{t+1}^T \widehat{\mathbf{H}}(\mathbf{w}_t) \Delta_{t+1} \leq \Delta_{t+1}^T \widehat{\mathbf{H}}(\mathbf{w}_t) \Delta_t - \Delta_{t+1}^T \nabla F(\mathbf{w}_t) + \Delta_{t+1}^T F(\mathbf{w}^*)$. By the mean value theorem

$$\begin{aligned} &\nabla F(\mathbf{w}_t) - \nabla F(\mathbf{w}^*) \\ &= \left(\int_0^1 \nabla^2 F(\mathbf{w}^* + \tau(\mathbf{w}_t - \mathbf{w}^*)) d\tau \right) (\mathbf{w}_t - \mathbf{w}^*). \end{aligned}$$

we get

$$\begin{aligned} &\Delta_{t+1}^T \widehat{\mathbf{H}}(\mathbf{w}_t) \Delta_{t+1} \\ &\leq \Delta_{t+1}^T \widehat{\mathbf{H}}(\mathbf{w}_t) \Delta_t - \Delta_{t+1}^T \left(\int_0^1 \nabla^2 F(\mathbf{w}^* + \tau(\mathbf{w}_t - \mathbf{w}^*)) d\tau \right) \Delta_t \\ &= \Delta_{t+1}^T \widehat{\mathbf{H}}(\mathbf{w}_t) \Delta_t - \Delta_{t+1}^T \nabla^2 F(\mathbf{w}_t) \Delta_t \\ &\quad + \Delta_{t+1}^T \nabla^2 F(\mathbf{w}_t) \Delta_t - \Delta_{t+1}^T \left(\int_0^1 \nabla^2 F(\mathbf{w}^* + \tau(\mathbf{w}_t - \mathbf{w}^*)) d\tau \right) \Delta_t \\ &\leq \|\Delta_{t+1}\| \left\| \widehat{\mathbf{H}}(\mathbf{w}_t) - \nabla^2 F(\mathbf{w}_t) \right\| \|\Delta_t\| \\ &\quad + \|\Delta_{t+1}\| \left(\int_0^1 \left\| \nabla^2 F(\mathbf{w}_t) - \nabla^2 F(\mathbf{w}^* + \tau(\mathbf{w}_t - \mathbf{w}^*)) \right\| d\tau \right) \|\Delta_t\| \\ &\leq \left\| \widehat{\mathbf{H}}(\mathbf{w}_t) - \nabla^2 F(\mathbf{w}_t) \right\| \|\Delta_t\| \|\Delta_{t+1}\| + \frac{M}{2} \|\Delta_t\|^2 \|\Delta_{t+1}\| \end{aligned}$$

Knowing that $\Delta_{t+1}^T \widehat{\mathbf{H}}(\mathbf{w}_t) \Delta_{t+1} \geq \lambda_{\min}(\widehat{\mathbf{H}}(\mathbf{w}_t)) \|\Delta_{t+1}\|^2$ and $\widehat{\mathbf{H}}(\mathbf{w}_t)$ is assumed to be positive definite, the result follows.

6.4 Proof of Lemma 4

With Lemma 2, we know that $\left\| \widehat{\mathbf{H}}(\mathbf{w}_t) - \nabla^2 F(\mathbf{w}_t) \right\| \leq \epsilon \Psi \gamma$ and $\lambda_{\min}(\widehat{\mathbf{H}}(\mathbf{w}_t)) \geq (1 - \epsilon \Psi) \gamma$, the result follows by applying these to Lemma 8.

6.5 Proof of Theorem 5

By choosing ϵ based on this requirement, with lemma 4, we have $\|\mathbf{w}_{t+1} - \mathbf{w}^*\| \leq \nu \|\mathbf{w}_t - \mathbf{w}^*\| + \eta \|\mathbf{w}_t - \mathbf{w}^*\|^2$ for every t . By requiring that $\nu \|\mathbf{w}_0 - \mathbf{w}^*\| + \eta \|\mathbf{w}_0 - \mathbf{w}^*\|^2 \leq \rho \|\mathbf{w}_0 - \mathbf{w}^*\|$, the result follows. The probability that all previous iterations success is the complement of the probability that at least one iteration fails, which is bounded by $t_0 \delta$ (Boole's inequality). Therefore, the probability of a successful process is at least $(1 - t_0 \delta)$.